

GRU-TV: Time- and velocity-aware GRU for patient representation on multivariate clinical time-series data

Ningtao Liu^{1,2}, Ruoxi Gao³

¹Key Laboratory of Intelligent Perception and Image Understanding of Ministry of Education, School of Artificial Intelligence, Xidian University, Xi'an 710071, China
nt.liu@stu.xidian.edu.cn

²Robarts Research Institute, Western University, London, ON, Canada, N6A 5B7
nliu258@uwo.ca

³University of Michigan, Ann Arbor, MI, 48109
gruoxi@umich.edu

Abstract

Electronic health records (EHRs) provide a rich repository to track a patient's health status. EHRs seek to fully document the patient's physiological status, and include data that is high dimensional, heterogeneous, and multimodal. The significant differences in the sampling frequency of clinical variables can result in high missing rates and uneven time intervals between adjacent records in the multivariate clinical time-series data extracted from EHRs. Current studies using clinical time-series data for patient characterization view the patient's physiological status as a discrete process described by sporadically collected values, while the dynamics in patient's physiological status are time-continuous. In addition, recurrent neural networks (RNNs) models widely used for patient representation learning lack the perception of time intervals and velocity, which limits the ability of the model to represent the physiological status of the patient.

In this paper, we propose an improved gated recurrent unit (GRU), namely time- and velocity-aware GRU (GRU-TV), for patient representation learning of clinical multivariate time-series data in a time-continuous manner. In proposed GRU-TV, the neural ordinary differential equations (ODEs) and velocity perception mechanism are used to perceive the time interval between records in the time-series data and changing rate of the patient's physiological status, respectively. Experimental results on two real-world clinical EHR datasets (PhysioNet2012, MIMIC-III) show that GRU-TV achieve state-of-the-art performance in computer aided diagnosis (CAD) tasks, and is more advantageous in processing sampled data.

INTRODUCTION

With continual advancements of informatization and digitization, many fields have recorded and accumulated multitude of time-series data, including health care [10], climate analysis [11] and quantitative investment [30]. According to the Healthcare Cost and Utilization Project (HCUP) of the National Inpatient Sample (NIS), in 2018, more than 7 million patients in the United States were hospitalized, and over 10 million medical records are generated¹. Clinically, clinician decisions on treatment and diagnosis of diseases rely

heavily on the individual patient's medical records, such as lab tests, previous procedures, medications, and diagnoses. Therefore, these rich medical records provide an opportunity for computer assist diagnosis (CAD) applications, specifically with machine learning methods.

Recently, there has been research focused on clinical needs using patient representation learning, such as patient subtyping [1, 3, 32], mortality prediction [12, 23, 29, 31], length-of-stay prediction [22, 23, 29], 24-hour decompensation [23, 26, 29], and multi-task learning [8]. Recurrent neural networks (RNNs) can share weights between layers, which allows them to be suitable for modeling sequence data of variable length. Therefore, RNN and its variant models like long-short term memory (LSTM), and gate recurrent unit (GRU) are widely used for patient representation learning with time-series data among these previous studies.

Health care data extracted from electronic health records (EHRs) are usually high-dimensional, heterogeneous, and multimodal [21], since the data points in EHRs are typically collected from different resources, such as medical sensors and examination procedures. The observation frequency varies widely across variables in these health care data, and some values are randomly or intentionally omitted, which results in the irregular sampling intervals and data sparsity in medical time-series data. However, a basic assumptions of RNNs is that the elapsed time between the adjacent records of time-series data are consistent, which makes RNNs inherently flawed in patient representation learning using clinical multivariate time-series data generated after time alignment of data points in EHRs.

Improved RNN models [1, 28] adapt to clinical time-series data by augmenting the input with a time interval. These methods require nonlinear mapping of time intervals as extended input to the RNN unit, and treat the patient's physiological status as a discrete process. The RNNs with decay term proposed in [2, 4] decay the hidden state in forward propagation by the time decay term, which was proven not to improve performance over standard RNN in [15]. How to update the hidden state of an RNN in a time-continuous manner? Some methods have tried to apply ordinary differential equation (ODE) to RNN for process-

¹<https://www.hcup-us.ahrq.gov/db/nation/nis/nissummstats.jsp>

ing non-uniformly sampled time-series data [7, 19] after the neural ODE was proposed in [6]. These methods are more flexible but require solving for the ODE of hidden state and lack intuition.

In addition, instantaneous vital sign rates are related to physiological dynamics and are important indicators of the human health condition [33]. thus, perception of changes in a patient’s physical condition is also critical for patient representation learning. However, current RNN models, whether representing a patient’s physiological status in a continuous or discrete manner, lack the ability to perceive the changes of patient’s physiological status.

In this paper, we propose a Time- and Velocity-aware GRU (GRU-TV) for patient representation based on GRU. In the proposed GRU-TV, the update of the hidden state and the forward propagation of the RNN in the time dimension are two parallel veins that interact through the ODE of the hidden state and the time interval between adjacent records. Inspired by neural ODE, the forward propagation of hidden states between timestamps is improved so as to perform patient representation learning in a time-continuous manner with unevenly sampled clinical multivariate time-series data and with the ability to perceive variable time intervals between adjacent records in the sequence. Besides, the velocity prediction is applied by expanding the instantaneous rate of hidden state as the input compared with standard GRU.

We hypothesize that our approach is not limited to GRU but can be applied to all existing RNN and its variants as a plug-and-play plugins, which allows feeding sporadic records into a time-continuous dynamics representation of patient’s physiological status evolution. This model is task-independent and can be applied to the learning patient representation of various tasks, including, phenotyping, in-hospital mortality prediction, length-of-stay prediction, etc. We conduct extensive experiments on Physionet2012 and MIMIC-III datasets, GRU-TV outperforms existing benchmarks, Comparisons with baseline models and ablation experimental results demonstrate that both the time-interval and velocity-aware mechanisms in our proposed GRU-TV have gains for patient representation learning. The intuitiveness and effectiveness shall benefit further technology and clinical research.

RELATED WORK

Related works using deep learning models for patient representation learning, such as length of stay prediction [18], in-hospital mortality prediction [13], patient phenotyping [1], and international classification of diseases (ICD) code classification [17] follow a similar paradigm of modeling clinical time-series data with a deep learning model following a task-specific output layer. Therefore, the design of deep learning model used for patient representation based on EHR is critical for the performance.

Modeling of EHR data In [20], a clinical decision support system using only the heart rate signal was developed. More studies, however, often use multimodal data to perform diverse clinical-assisted decision-making tasks and improve the prediction accuracy. Other work has proposed unstructured text records and waveform data for Patient rep-

resentation in addition to the sporadically recorded structured data in the EHR. In [29], electrocardiogram (EGG) data is integrated with discrete clinical events to predict the decompensation and length of stay. This high-density data are embedded into low-dimensional representations by convolutional neural networks (CNN), and the multi-channel attention is used to assign weights to high-density EGG and various clinical variables in a learning style. In [18, 27], both narrative text and numerical records were used for the prediction of in-hospital mortality, 30-day unplanned readmission, and prolonged length of stay. Specifically, a sequence of time-ordered tokens throughout the patient’s records from the beginning of recording until the point of prediction is formed by splitting the medical event data in each attribute into discrete values, splitting the clinical note text into a sequence of tokens, and normalizing the numeric values in [18]. While in [27], a similar approach is used for numerical measurements and lab values, clinical notes, and static demographics, after which these numerical multimodal data were formed into a structured patient record.

Perception of uneven time intervals Uneven time interval between two adjacent records in the time-series sequence is another characteristic of clinical multivariate time-series data, which results from differences in data modality (e.g., waveform data, text of medical prescriptions, and medical examination result values), and observation frequency. The changing rate of variables in real-world data, especially in clinical scenarios, is also an important consideration for making correct decisions. However, basic RNNs do not have the ability to perceive the time interval between two adjacent records, i.e. the time interval between records in the sequence and the changing rates of the variables are assumed to be consistent by default. Based on the assumption that the longer the time interval, the lower the reliability of the memory inherited by the RNN from the previous moment, T-LSTM proposed in [1] uses the time interval between adjacent records after a nonlinear mapping (monotonically decreasing function) as a discounting factor for the short-term memory of the previous timestep accepted by the LSTM unit. In DeepCare [16], the time parameterization is introduced to handle irregular timing by modifying the forget gate. The study [14] shows another route to improve the forward propagation between adjacent units of the RNN along the neural ODE proposed in [5] so that it possesses the ability to perceive uneven time intervals between records in a sequence.

Patient representation learning. In terms of methods, deep learning models are increasingly used in patient representation learning tasks. These models are generally generic, i.e., task-independent, focusing on the representation of the patient’s physiological condition from clinical time-series data extracted from the EHR. Many studies have tried different methods to improve the basic RNN model to adapt to the sparsity, high dimensionality and inhomogeneity of clinical time series data. In [13], L Lei, et.al applied a recurrent neural network-based denoising autoencoder to encode patient’s hospital record into a low-dimensional dense vector. Considering the varying length of patients’ EHRs, the non-negative tensor factorization models the input sequence

to a temporal tensor and serves as the input to the LSTM. In addition to RNNs, convolutional neural networks (CNNs) are also used for patient representation learning tasks. Compared with RNN, CNN cannot handle sequence data of indefinite length, so it needs to pre-process the input sequence. In [25], the patient visit sequence data is used as input to the CNN after being padded to a fixed length, while in [29], CNN is used to extract features from the dense ECG waveform and as part of the input to the RNN model. In terms of tasks, deep representation models can be followed by task-specific output layers for various clinical tasks, such as mortality prediction [18], length-of-stay prediction [34], patient subtyping [1], medical cost [24] etc.

DATA DESCRIPTION

Medical time-series data from EHR contain multiple variables to describe the physiological status of the patients with different dimensions, and more abundance in types and modalities of clinical variables in the intensive care unit (ICU). The way these variables are obtained is highly variable, i.e., the sampling frequencies of waveform data (e.g., electrocardiogram) are higher than 30 Hz, blood gases (e.g., oxygen saturation, partial pressure of oxygen) are often performed every 10 minutes, vital signs (heart rate, pH, and respiratory rate) are performed every 5 minutes, respectively, and demographic informations (e.g., height, gender, and age) are recorded only once during an admission. Furthermore, manual recording often causes random missing variables.

As shown in Figure 1 for a ICU stay sample extracted from MIMIC-III by pipeline provided in [8], the clinical variables in the sequence are missing to varying degrees, and even some clinical variables (e.g., FiCO_2) are completely missing. The mean and standard deviation of the missing rate for each clinical variable obtained from the statistics of all ICU stays are shown in Figure 2, in which the missing rate of these clinical variables is usually higher than 0.5, or even higher than 0.9.

Another significant characteristic is that the elapsed time between two records in the sequence is not uniform. The mean and standard deviation of the time interval between adjacent records at different sampling rates for the PhysioNet2012 and MIMIC-III datasets used in this paper are shown in Figure 3. This inhomogeneity is also caused by differences in the timing and frequency of individual variable acquisitions, so aligning the values of the variables according to time manifests itself as an uneven time interval between records.

In this paper, we describe a clinical time series S with a length of n as a set containing n records x , i.e., $S = \{x_1, x_2, \dots, x_n\}$, $|S| = n$. Given D_r is the dimension of time series data, record $x_i \in \mathbb{R}^{D_r}$ can be described as the set of clinical variables that are observed at the time t_i . The elapsed time between two adjacent records is defined as $\Delta t_i = t_i - t_{i-1}$, $\Delta t_1 = 1$ which is not assumed consistent in this study. The record x_{t_i} is also not assumed to contain complete clinical variables, i.e. $|x_{t_i}| \leq D_r$.

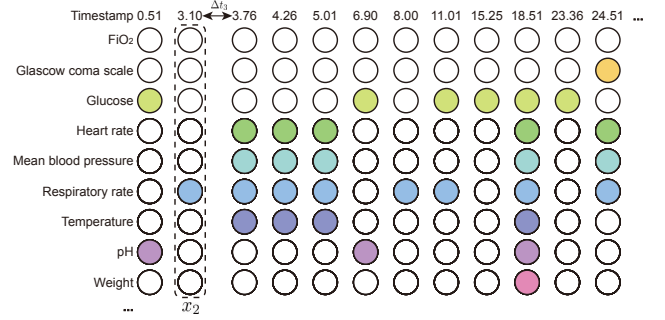


Figure 1: A sample of clinical multivariate time series data extracted from MIMIC-III. Without loss of generality, the variables and timestamps in the sequence are sampled. The colored circles indicate that the corresponding variable has real value collected at that timestamp, while the gray circles indicate that the variable is missing. The timestamp is a relative time generated from the time the patient was admitted to the ICU as the starting time point.

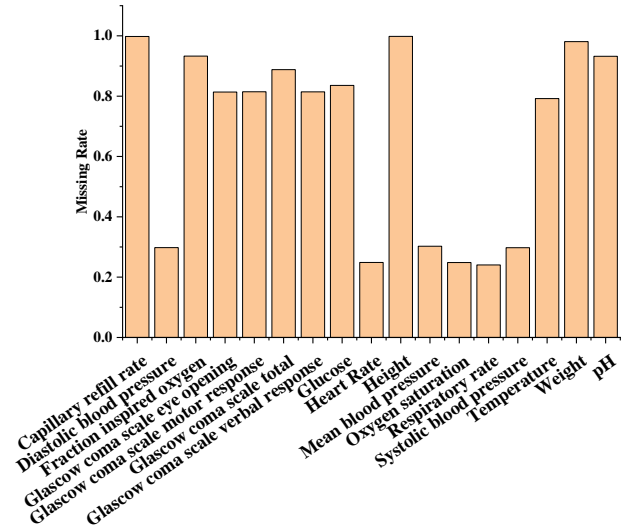


Figure 2: The missing rates of the clinical variables.

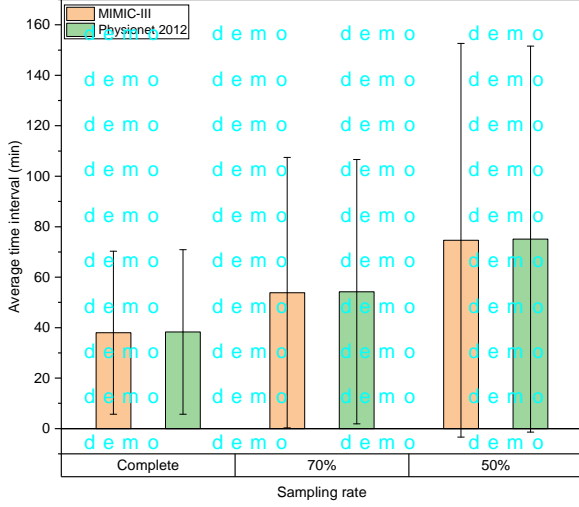


Figure 3: Mean and standard deviation of the elapsed time (minutes) between adjacent records at different sampling rates for the datasets extracted from PhysioNet2012 and MIMIC-III.

METHODOLOGY

The overall structure of GRU-TV is shown in Figure 4. It contains two main components based on GRU, which will be described below: the time interval perception to perceive the time interval between adjacent records in the sequence, and the velocity perception to perceive the velocity at which the physiological status representation of the patient corresponding to the input sequence changes. Our approach is not limited to GRU, but can be applied to any RNN model alive and its variants as a plug-and-play plugin.

Missing value preprocessing

As mentioned in Section , there are a large number of missing value in clinical multivariate time-series data, and GRU takes fixed-length vectors as input, so data padding is widespread in this data. The missing variables in the series are filled with the latest value, that is, the actual value of the filled variable in the previous collection is used as the filling value (if the record is missing at the beginning of the series, the default value of the variable is used as the real value). However, a large number of filling values introduce noise into the input data and change the inherent distribution of the variable, so the filling and real values should be distinguished so that the GRU can perceive the difference.

In GRU-TV, we expand the input of the basic standard GRU to include the variable mask vector corresponding to the input record as well. The forward propagation of the standard GRU is modified as follows:

$$\begin{aligned}
 r_i &= \sigma(W_r[x_i, h_{i-1}, m_i] + b_r) \\
 z_i &= \sigma(W_z[x_i, h_{i-1}, m_i] + b_z) \\
 g_i &= \tanh(W_g[x_i, r_i \odot h_{i-1}, m_i]) \\
 h_i &= z_i \odot h_{i-1} + (1 - z_i) \odot g_i
 \end{aligned} \tag{1}$$

where W_r , W_z , and $W_g \in \mathbb{R}^{(D_r \times 2 + D_h) \times D_h}$ are the weights of GRU, b_r , b_z and $b_g \in \mathbb{R}^{D_h}$ are the bias of GRU, $\sigma(\cdot)$ is sigmoid activate function, and \odot is element-wise multiplication.

Time interval perception

For a sequence with length n , RNNs such as GRU update the hidden state by combining the transformation of the previous hidden state and the current input record:

$$h_{i+1} = GRU(h_i, x_i, \theta_i) \tag{2}$$

where $i \in \{0, \dots, n\}$ and $h_i \in \mathbb{R}^{D_h}$. This transformation is discrete and does not take into account the time interval between adjacent records, and therefore has natural drawbacks for patient representation learning using multivariate clinical data. To solve this deficiency, we would like GRU to update the hidden attitude as follows:

$$h_{i+1} = GRU'(h_i, x_i, t_i, t_{i-1}, \theta_i) \tag{3}$$

where t_i and t_{i-1} are the timestamps of records x_i and x_{i-1} , respectively.

Inspired by the neural ordinary differential equations proposed in [6], instead of expanding an additional elapsed time as the input to the GRU cell, we keep the forward propagation of the standard GRU cell unchanged in this step but improve the update method of the hidden state h_t after the cell receives a record. In the proposed GRU-TV, the hidden representation h_n is not fed into GRU directly in the next timestep, but we obtain the difference equation for h_t :

$$\begin{aligned}
 \Delta h_i &= h_i - h_{i-1} \\
 &= (1 - z_i) \cdot (g_i - h_{i-1})
 \end{aligned} \tag{4}$$

which leads to the update of h_i

$$h_i = h_{i-1} + \Delta t_i \cdot \Delta h_i \tag{5}$$

where $\Delta t_i = t_i - t_{i-1}$ is the elapsed time of x_i and x_{i-1} .

Velocity interval perception

In clinical practice, the transient rate of vital signs associated with physiological kinetics is an important indicator of a patient's physiological status. Therefore, in the proposed GRU-TV, the ordinary differential equations (ODE) of the hidden state is also used as an input thus giving the GRU the ability to perceive the velocity. How to parameterize the transient rate of patient's physical condition by GRU? As proved in [6, 7], when the time interval between adjacent records is infinitesimal, the limiting form of the hidden state in Section , i.e., its ordinary differential equation (ODE) is:

$$\frac{dh(t)}{dt} = (1 - z(t)) \cdot (g(t) - h(t)) \tag{6}$$

The ODE of h_t stays within the $[-1, 1]$ range, which guarantees the convergence of our model.

Although the instantaneous rate of h exists, we still use its discrete form as an input to GRU in this study:

$$\begin{aligned}
 r_i &= \sigma(W_r[x_i, h_{i-1}, m_i, \Delta h_i] + b_r) \\
 z_i &= \sigma(W_z[x_i, h_{i-1}, m_i, \Delta h_i] + b_z) \\
 g_i &= \tanh(W_g[x_i, r_i \odot h_{i-1}, m_i, \Delta h_i] + b_g) \\
 \Delta h_i &= (1 - z_i) \cdot (g_i - h_{i-1})
 \end{aligned} \tag{7}$$

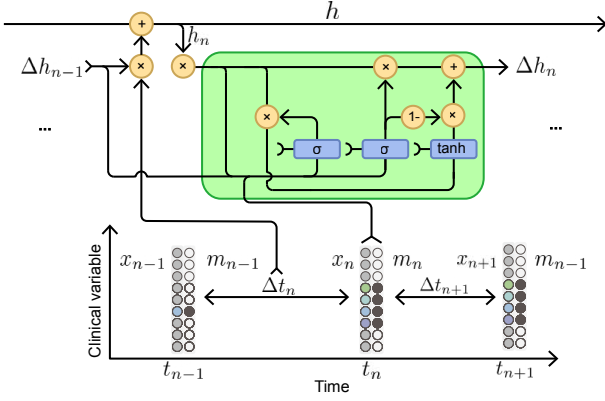


Figure 4: Illustration of the proposed GRU-T unit

where $\Delta h_i \in \mathbb{R}^{D_h}$ is the discrete form of dh , which is defined earlier, W_r , W_z , and $W_g \in \mathbb{R}^{(D_r \times 2 + D_h \times 2) \times D_h}$ are the weight.

It is worth noting that here we use the rate of the hidden state rather than the input variable as the input to the velocity perception module. The reason for this is that the velocity of the input variable cannot be accurately obtained because there are a large number of filled values in input sequence, while the hidden state can better represent the patient's physiological condition.

Loss function

The hidden attitudes obtained after traversing the entire input sequence are fed into a task-specific separator, which in this study is a fully-connected neural network with a sigmoid function as the activation function. Binary cross entropy loss (BCE) loss was selected as the loss function since the experiments in this study are multi-label binary classification tasks. The BCE loss is defined as:

$$\mathcal{L} = \frac{1}{K} \sum_{k=1}^K y_k \cdot \log(\hat{y}_k) + (1 - y_k) \cdot \log(1 - \hat{y}_k) \quad (8)$$

where $y_k \in \{0, 1\}$ is the label of k^{th} binary classification task, and $\hat{y} \in (0, 1)$ is the predicted probability of k -th classification task.

EXPIREMENT

Comparing model

We compare our proposed method to the following deep learning methods: GRU-Standard, GRU-Decay [4], LSTM [9], and T-LSTM [1]. We take the only-time-aware included model (GRT-T) as a comparison model and the γ_h and γ_x used in GRU-Decay are also embedded in GRU-T respectively for more comprehensive comparisons. For GRU-T- γ_h , the h_i calculated in Equation 1 is modified by γ_h :

$$\begin{aligned} \gamma_{h_i} &= e^{\{-\max(0, W_{\gamma_h} \delta_t + b_{\gamma_h})\}} \\ h_i &\leftarrow h_i \gamma_{h_i} \end{aligned} \quad (9)$$

where δ_t is a vector containing the elapsed time of last collection for every variable. For GRU-T- γ_x , the trainale decay coefficient are applied in the filling of the missing values in record x_t , Equation ?? is implemented by

$$\begin{aligned} \gamma_{x_i} &= e^{\{-\max(0, W_{\gamma_x} \delta_i + b_{\gamma_x})\}} \\ \hat{x}_t^d &= m_i^d x_i^d + (1 - m_i^d) (\gamma_{x_i}^d x_{last}^d + (1 - \gamma_{x_i}^d) \tilde{x}^d) \end{aligned} \quad (10)$$

where \tilde{x}^d is the default value of d -th (the average of real value is used as default in this study). For GRU-T- γ_{h+x} , both the γ_h and γ_x in GRU-Decay are applied in GRU-T. All the mdoels were implemented in PyTorch, and mini-batch stochastic Adam optimizer was used.

Dataset

We demonstrate the performance of our proposed models on two real-world EHR datasets: PhysioNet2012² and MIMIC-III³, and both of them are publicly available.

PhysioNet2012 is a dataset for the PhysioNet Computing in Cardiology Challenge 2012. This multivariate clinical time series dataset consists of record from 12,000 ICU stays, all patients were adults who were admitted for a wide variety of reasons to cardiac, medical, surgical, and trauma ICUs. ICU stays less than 48 hours have been excluded in this study.

MIMIC-III is a large, freely-available dataset comprising health-related data associated with over 40,000 patients who stayed in critical care units of the Beth Israel Deaconess Medical Center between 2001 and 2012. Over 58,000 hospital admission records were collected in this dataset. In this study, two multi-task classifications including acute phenotype classification and ICD-9 diagnosis categories classification tasks were performed using this datasets.

To evaluate the performance of the proposed model under low sampling rate situations, we sampled the records in the input sequences at 70% and 50% sampling rare, which yields simulation data with more uneven time intervals between records.

For each dataset, after organizing the sporadically recorded data points into multivariate time series S , the variable time interval sequence and mask sequence corresponding to S were obtained by referring to the method in GRU-Decay [4], are noted as Δ and M , respectively. In addition, the elapsed time between adjacent records x_{t_i} and $x_{t_{i-1}}$ in the elapsed time sequence required for GRU-T were obtained by the difference between the corresponding time points t_i and t_{i-1} , where the elapsed time between x_1 and the previous record was set to 1.

Experimental Setup

To permit a fair comparison between the methods, consistent hyperparameters, network setting, training pipeline, and dataset splits were used for all the deep learning methods. The training was stopped if the number of training epoch is greater than 30 and there is no performance improvement

²<https://www.physionet.org/content/challenge-2012/1.0.0/>

³<https://mimic.mit.edu/>

on the validation set for 3 consecutive iterations. The parameters with the best validation performance were selected to evaluate the performance on test dataset. The final performance was the average of three independent test performances. Area under the ROC curve (AUROC) and area under the precision-recall curve (AUPRC) were the comparison metrics for this paper, since all tasks are classification in this paper. The macro average AUC were also calculated for the multi-task classification.

The hidden states, obtained after traversing all records in the input sequence, are fed to a fully connected layer to obtain predictions. The activation functions are task-specific, sigmoid is used for multi-label binary classification, and softmax is used for multi-category classification.

Multi-task classification on PhysioNet2012

In this study, we used PhysioNet2012 data set for multi-task classification, which contains four sub-tasks: in-hospital mortality prediction, length-of-stay less than three days binary classification, patient had cardiac condition binary classification, and patient recovered from surgery prediction binary classification.

In this task, the non-sequential variables in the dataset were discarded due to the basic GRU unit requires the input of timing data. The variables of the time series were reorganized, in which variables collected at the same point in time or those collected at intervals of less than 5 minutes were included in the same record.

Table 1 depicts the experimental results on the multi-task classification of PhysioNet2012 dataset. For each metric, the best and second best are marked in bold and underlined, respectively.

In general, the application of ODE significantly improves the performance of the baseline approach for each subtask, and this improvement is more obvious on the sampled simulation data. When the complete data was used for the experiment, the performances of GRU-Decay are the best on the two sub-tasks of cardiac classification and surgery classification. In other tasks, the GRU-T model combined with γ_h and γ_x or the GRU-T models could achieve performance that exceeds that of GRU-Decay. On all but two subtasks cardiac classification and surgery classification, GRU-T variant models, which combines γ_h , γ_x , or both γ_h and γ_x proposed in GRU-Decay, have the best performance and macro average AUCROC. However, when simply comparing GRU-T and GRU-Decay, the former has a more pronounced improvement relative to the GRU-Standard model. GRU-TV has an advantage over the baseline model but is not significant and is not superior to GRU-T.

In the sampled datasets, perception of the elapsed time between records is more important since random sampling results in a more uneven time interval between records in a sequence. The importance of the ability to perceive the unevenness of the time interval between records can be demonstrated by the improved performance of T-LSTM and GRU-T on each subtask relative to the other models. Except for the length of stay classification subtask, applying the γ_h and γ_x terms in GRU-Decay in the GRU-Standard and GRU-T can even have a negative impact on the performance of the

base model, and this negative impact is more obvious on the GRU-Standard. GRU-TV performs significantly better relative to the other models. On the dataset sampled at 70% sampling rate, GRU-TV significantly outperforms the other models on all subtasks, with the average AUC improving by 2.8% relative to the suboptimal T-LSTM and by 2.3% relative to the suboptimal GRU-T on the 50% sampling rate dataset.

It should be noted that the performances of GRU-T and T-LSTM are very close in the sampled datasets, so the average AUCs of them. But in the complete dataset, the GRU-T and its variants perform much better than other models. The mean values of macro average AUC for the GRU-T and T-LSTM in the three data sets are 0.8253 and 0.8360, respectively, which show our proposed GRU-T model is generalizable and robust on both sampled and complete datasets.

Acute phenotype classification on MIMIC-III

In the ICU setting, acute illnesses with short onset cycles and diagnostic time windows are more difficult to diagnose clinically and require more rapid intervention and treatment. In this paper, we use the proposed model to perform subtyping of acute phenotype commonly seen in clinic. Continue...

ICD-9 diagnosis categories classification on MIMIC-III

*

CONCLUSION

In this paper, we proposed a GRU variant unit for modeling clinical multivariate time-series data, called GRU-T. GRU-T improves the forward propagation between adjacent GRUs through the ODE of hidden state to continuously represent the changing process of the patient's physiological status, and further, enables GRU the ability to perceive the speed and time interval of changes in relevant clinical variables.

Compared to RNN models such as GRU and LSTM, GRU-T allows the time interval between records of the input sequence to be of free length, and eliminating the need for imputation. GRU-T achieves state-of-the-art results on multiple tasks on both real-world datasets, especially on sampled simulated data. Importantly, the hidden state ODE in GRU-T can be used as a plug-and-play plugin in other RNN models and achieve performance improvement, as shown in our experimental results applying it to the GRU-D model. In our future work, it will be applied to other specific tasks of patient characterization with clinical time-series data, to embed it in online real-time alert systems to improve computer aided diagnostics, and to evaluate the generalizability of our model with real-world data.

Subsequent work will be interpretable studies of adjunctive therapy and patient representational learning.

ACKNOWLEDGMENT

*

Table 1: Performances comparison of methods on multi-task classification of complete PhysioNet2012 dataset, and sampled PhysioNet2012 dataset with 70% and 50% sampling rate. AUROC: area under the receiver operating characteristic curve, AUPRC: area under the precisionrecall curve, Mor: in-hospital mortality, LoS: length-of-stay less than 3 days, Car: whether the patient had a cardiac condition, Sur: whether the patient was recovering from surgery, Mac: macro average AUCROC. The best and second best performance for each subtask as well as the average are bolded and underlined.

Sampling Rate	Method	AUROC				
		Mor	LoS	Car	Sur	Mac
100%	GRU-Standard	0.8638	0.8043	<u>0.9510</u>	0.8956	0.8787
	GRU-Decay	0.8601	0.8199	0.9525	0.9043	0.8842
	T-LSTM	0.8469	0.7639	0.9274	0.8735	0.8529
	GRU-T- γ_h	0.8641	0.8432	0.9507	0.8992	0.8893
	GRU-T- γ_x	<u>0.8667</u>	0.8200	0.9497	0.8947	0.8827
	GRU-T- γ_{h+x}	0.8864	0.8086	0.9438	0.8980	0.8842
	GRU-T	0.8619	0.8255	0.9499	0.9019	<u>0.8848</u>
	GRU-TV	0.8498	<u>0.8380</u>	0.9475	<u>0.9028</u>	0.8845
70%	GRU-Standard	0.6709	0.7254	0.9170	0.8046	0.7795
	GRU-Decay	0.6488	0.7774	0.8492	0.7461	0.7554
	T-LSTM	<u>0.7512</u>	<u>0.7924</u>	0.9097	<u>0.8215</u>	<u>0.8187</u>
	GRU-T- γ_h	0.7371	0.7808	0.8987	0.8074	0.8060
	GRU-T- γ_x	0.7085	0.7699	0.8914	0.8063	0.7940
	GRU-T- γ_{h+x}	0.7449	0.7716	0.9026	0.8005	0.8049
	GRU-T	0.7505	0.7698	<u>0.9194</u>	0.8135	0.8133
	GRU-TV	0.7891	0.8017	0.9208	0.8539	0.8413
50%	GRU-Standard	0.7132	0.7160	0.8957	0.8102	0.7838
	GRU-Decay	0.7426	0.7857	0.8819	0.8093	0.8049
	T-LSTM	0.7666	0.7082	<u>0.9133</u>	<u>0.8291</u>	0.8043
	GRU-T- γ_h	0.7425	0.7357	0.8942	0.8062	0.7946
	GRU-T- γ_x	0.7222	0.7395	0.9013	0.8026	0.7914
	GRU-T- γ_{h+x}	0.7248	<u>0.7724</u>	0.9032	0.8122	0.8031
	GRU-T	0.7453	0.7712	0.9045	0.8183	<u>0.8098</u>
	GRU-TV	0.7792	0.7683	0.9193	0.8467	0.8283

Table 2: Performances comparison of acute phenotype classification using complete sequences, and sampled sequences with 70% and 50% sampling rate extracted from MIMIC-III dataset. AURF: acute and unspecified renal failure, ACD: acute cerebrovascular disease, PC: pulmonary collapse, PN: pneumonia RF: respiratory failure, SE: septicemia, SH: shock. The best and second best performance for each subtask as well as the average are bolded and underlined.

Sampling Rate	Method	AUPRC							
		AURF	ACD	PC	PN	RF	SE	SH	MACRO
100%	GRU-Standard	0.7619	0.8830	0.6746	0.7835	0.8710	0.8070	0.8621	0.8061
	GRU-Decay	0.7630	0.9050	0.6901	0.7909	0.8794	0.8098	0.8577	0.8137
	T-LSTM								
	GRU-T- γ_h								
	GRU-T- γ_x								
	GRU-T- γ_{h+x}								
	GRU-T	0.7567	0.8717	0.6726	0.7892	0.8733	0.8052	0.8582	0.8039
	GRU-TV								
70%	GRU-Standard								
	GRU-Decay								
	T-LSTM	0.7059	0.7928	0.6551	0.7576	0.8241	0.7687	0.8201	0.7606
	GRU-T- γ_h								
	GRU-T- γ_x								
	GRU-T- γ_{h+x}								
	GRU-T								
	GRU-TV	0.7493	0.8647	0.6725	0.8002	0.8796	0.8075	0.8527	0.8102
50%	GRU-Standard								
	GRU-Decay								
	T-LSTM	0.6984	0.7918	0.6546	0.7435	0.8234	0.7587	0.8218	0.7560
	GRU-T- γ_h								
	GRU-T- γ_x								
	GRU-T- γ_{h+x}								
	GRU-T								
	GRU-TV	0.7409	0.8621	0.6675	0.7845	0.8638	0.7941	0.8439	0.7938

References

- [1] Baytas, I. M.; Xiao, C.; Zhang, X.; Wang, F.; Jain, A. K.; and Zhou, J. 2017. Patient subtyping via time-aware lstm networks. In *Proceedings of the 23rd ACM SIGKDD international conference on knowledge discovery and data mining*, 65–74. (document)
- [2] Cao, W.; Wang, D.; Li, J.; Zhou, H.; Li, L.; and Li, Y. 2018. Brits: Bidirectional recurrent imputation for time series. *Advances in neural information processing systems* 31. (document)
- [3] Che, Z.; Kale, D.; Li, W.; Bahadori, M. T.; and Liu, Y. 2015. Deep computational phenotyping. In *Proceedings of the 21th ACM SIGKDD International Conference on Knowledge Discovery and Data Mining*, 507–516. (document)
- [4] Che, Z.; Purushotham, S.; Cho, K.; Sontag, D.; and Liu, Y. 2018. Recurrent neural networks for multivariate time series with missing values. *Scientific reports* 8(1): 1–12. (document)
- [5] Chen, R. T.; Rubanova, Y.; Bettencourt, J.; and Duvenaud, D. K. 2018. Neural ordinary differential equations. *Advances in neural information processing systems* 31. (document)
- [6] Chen, R. T. Q.; Rubanova, Y.; Bettencourt, J.; and Duvenaud, D. K. 2018. Neural Ordinary Differential Equations. In *Advances in Neural Information Processing Systems*, volume 31. Curran Associates, Inc. (document)
- [7] De Brouwer, E.; Simm, J.; Arany, A.; and Moreau, Y. 2019. Gru-ode-bayes: Continuous modeling of sporadically-observed time series. *arXiv preprint arXiv:1905.12374*. (document)
- [8] Harutyunyan, H.; Khachatrian, H.; Kale, D. C.; Ver Steeg, G.; and Galstyan, A. 2019. Multitask learning and benchmarking with clinical time series data. *Scientific data* 6(1): 1–18. (document)
- [9] Hochreiter, S.; and Schmidhuber, J. 1997. Long short-term memory. *Neural computation* 9(8): 1735–1780. (document)
- [10] Johnson, A. E.; Pollard, T. J.; Shen, L.; Li-Wei, H. L.; Feng, M.; Ghassemi, M.; Moody, B.; Szolovits, P.; Celi, L. A.; and Mark, R. G. 2016. MIMIC-III, a freely accessible critical care database. *Scientific data* 3(1): 1–9. (document)
- [11] Jones, D. A.; Wang, W.; and Fawcett, R. 2009. High-quality spatial climate data-sets for Australia. *Australian Meteorological and Oceanographic Journal* 58(4): 233. (document)
- [12] Kemp, J.; Rajkomar, A.; and Dai, A. M. 2019. Improved Hierarchical Patient Classification with Language Model Pretraining over Clinical Notes. *arXiv preprint arXiv:1909.03039*. (document)
- [13] Lei, L.; Zhou, Y.; Zhai, J.; Zhang, L.; Fang, Z.; He, P.; and Gao, J. 2018. An effective patient representation learning for time-series prediction tasks based on EHRs. In *2018 IEEE International Conference on Bioinformatics and Biomedicine (BIBM)*, 885–892. IEEE. (document)
- [14] Moe, S.; and Sterud, C. 2021. Decoupling dynamics and sampling: RNNs for unevenly sampled data and flexible online predictions. In *Learning for Dynamics and Control*, 943–953. PMLR. (document)
- [15] Mozer, M. C.; Kazakov, D.; and Lindsey, R. V. 2017. Discrete event, continuous time rnns. *arXiv preprint arXiv:1710.04110*. (document)
- [16] Pham, T.; Tran, T.; Phung, D.; and Venkatesh, S. 2016. Deepcare: A deep dynamic memory model for predictive medicine. In *Pacific-Asia conference on knowledge discovery and data mining*, 30–41. Springer. (document)
- [17] Purushotham, S.; Meng, C.; Che, Z.; and Liu, Y. 2018. Benchmarking deep learning models on large healthcare datasets. *Journal of biomedical informatics* 83: 112–134. (document)
- [18] Rajkomar, A.; Oren, E.; Chen, K.; Dai, A. M.; Hajaj, N.; Hardt, M.; Liu, P. J.; Liu, X.; Marcus, J.; Sun, M.; et al. 2018. Scalable and accurate deep learning with electronic health records. *NPJ Digital Medicine* 1(1): 1–10. (document)
- [19] Rubanova, Y.; Chen, R. T.; and Duvenaud, D. K. 2019. Latent ordinary differential equations for irregularly-sampled time series. *Advances in neural information processing systems* 32. (document)
- [20] Sadeghi, R.; Banerjee, T.; and Romine, W. 2018. Early hospital mortality prediction using vital signals. *Smart Health* 9: 265–274. (document)
- [21] Si, Y.; Du, J.; Li, Z.; Jiang, X.; Miller, T.; Wang, F.; Jim Zheng, W.; and Roberts, K. 2021. Deep Representation Learning of Patient Data from Electronic Health Records (EHR): A Systematic Review. *Journal of Biomedical Informatics* 115: 1–47. (document)
- [22] Si, Y.; and Roberts, K. 2019. Deep patient representation of clinical notes via multi-task learning for mortality prediction. *AMIA Summits on Translational Science Proceedings* 2019: 779. (document)
- [23] Song, H.; Rajan, D.; Thiagarajan, J.; and Spanias, A. 2018. Attend and diagnose: Clinical time series analysis using attention models. In *Proceedings of the AAAI Conference on Artificial Intelligence*, volume 32. (document)
- [24] Stojanovic, J.; Gligorijevic, D.; Radosavljevic, V.; Djuric, N.; Grbovic, M.; and Obradovic, Z. 2016. Modeling healthcare quality via compact representations of electronic health records. *IEEE/ACM transactions on computational biology and bioinformatics* 14(3): 545–554. (document)
- [25] Suo, Q.; Ma, F.; Yuan, Y.; Huai, M.; Zhong, W.; Gao, J.; and Zhang, A. 2018. Deep patient similarity learning for personalized healthcare. *IEEE transactions on nanobioscience* 17(3): 219–227. (document)

- [26] Suresh, H.; Gong, J. J.; and Gutttag, J. V. 2018. Learning tasks for multitask learning: Heterogenous patient populations in the icu. In *Proceedings of the 24th ACM SIGKDD International Conference on Knowledge Discovery & Data Mining*, 802–810. (document)
- [27] Suresh, H.; Hunt, N.; Johnson, A.; Celi, L. A.; Szolovits, P.; and Ghassemi, M. 2017. Clinical intervention prediction and understanding with deep neural networks. In *Machine Learning for Healthcare Conference*, 322–337. PMLR. (document)
- [28] Wang, T.; Qiu, R. G.; and Yu, M. 2018. Predictive modeling of the progression of Alzheimer’s disease with recurrent neural networks. *Scientific reports* 8(1): 1–12. (document)
- [29] Xu, Y.; Biswal, S.; Deshpande, S. R.; Maher, K. O.; and Sun, J. 2018. Raim: Recurrent attentive and intensive model of multimodal patient monitoring data. In *Proceedings of the 24th ACM SIGKDD international conference on Knowledge Discovery & Data Mining*, 2565–2573. (document)
- [30] Yang, X.; Liu, W.; Zhou, D.; Bian, J.; and Liu, T.-Y. 2020. Qlib: An AI-oriented Quantitative Investment Platform. *arXiv preprint arXiv:2009.11189*. (document)
- [31] Yin, K.; Qian, D.; Cheung, W. K.; Fung, B. C.; and Poon, J. 2019. Learning phenotypes and dynamic patient representations via rnn regularized collective non-negative tensor factorization. In *Proceedings of the AAAI Conference on Artificial Intelligence*, volume 33, 1246–1253. (document)
- [32] Zhang, Y.; Zhou, H.; Li, J.; Sun, W.; and Chen, Y. 2018. A Time-Sensitive Hybrid Learning Model for Patient Subgrouping. In *2018 International Joint Conference on Neural Networks (IJCNN)*, 1–8. IEEE. (document)
- [33] Zhao, H.; Hong, H.; Sun, L.; Li, Y.; Li, C.; and Zhu, X. 2017. Noncontact physiological dynamics detection using low-power digital-IF Doppler radar. *IEEE Transactions on Instrumentation and Measurement* 66(7): 1780–1788. (document)
- [34] Zhou, C.; Jia, Y.; Motani, M.; and Chew, J. 2017. Learning deep representations from heterogeneous patient data for predictive diagnosis. In *Proceedings of the 8th ACM International Conference on Bioinformatics, Computational Biology, and Health Informatics*, 115–123. (document)